JACS
JOURNAL OF THE AMERICAN CHEMICAL SOCIETY
Article
pubs.acs.org/JACS

Advanced Model Compounds for Understanding Acid-Catalyzed Lignin Depolymerization: Identification of Renewable Aromatics and a Lignin-Derived Solvent

Ciaran W. Lahive,[†] Peter J. Deuss,[‡] Christopher S. Lancefield,[†] Zhuohua Sun,[‡] David B. Cordes,[†] Claire M. Young,[†] Fanny Tran,[†] Alexandra M. Z. Slawin,[†] Johannes G. de Vries,[‡,§] Paul C. J. Kamer,[†] Nicholas J. Westwood,*[,†] and Katalin Barta*[,‡]

[†]School of Chemistry and Biomedical Science Research Complex, University of St Andrews and EaStCHEM, North Haugh, St Andrews, Fife KY16 9ST, United Kingdom

[‡]Stratingh Institute for Chemistry, University of Groningen, Nijenborgh 4, 9747 AG Groningen, The Netherlands

[§]Leibniz-Insitut für Katalyse e.V., Albert-Einstein-Straße 29a, 18059 Rostock, Germany

Supporting Information

ABSTRACT: The development of fundamentally new approaches for lignin depolymerization is challenged by the complexity of this aromatic biopolymer. While overly simplified model compounds often lack relevance to the chemistry of lignin, the direct use of lignin streams poses significant analytical challenges to methodology development. Ideally, new methods should be tested on model compounds that are complex enough to mirror the structural diversity in lignin but still of sufficiently low molecular weight to enable facile analysis. In this contribution, we present a new class of advanced (β-O-4)-(β-5) dilinkage models that are highly realistic representations of a lignin fragment. Together with selected β-O-4, β-5, and β–β structures, these compounds provide a detailed understanding of the reactivity of various types of lignin linkages in acid catalysis in conjunction with stabilization of reactive intermediates using ethylene glycol. The use of these new models has allowed for identification of novel reaction pathways and intermediates and led to the characterization of new dimeric products in subsequent lignin depolymerization studies. The excellent correlation between model and lignin experiments highlights the relevance of this new class of model compounds for broader use in catalysis studies. Only by understanding the reactivity of the linkages in lignin at this level of detail can fully optimized lignin depolymerization strategies be developed.

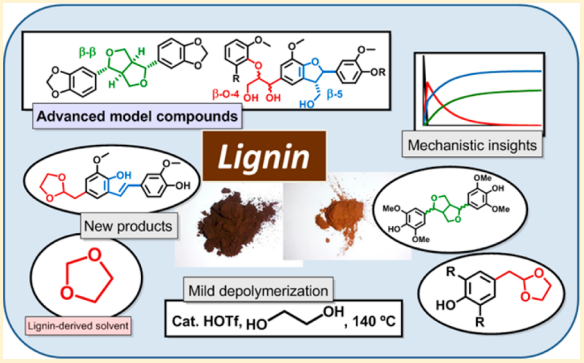

INTRODUCTION

The efficient depolymerization of lignin is one of the major challenges in the full valorization of renewable lignocellulose resources[1,2] and requires fundamentally new catalytic methods.[3,4] However, the development of new approaches is particularly challenging due to the complexity of this aromatic polymer.[2a,5] Methodology development is often done on overly simplified model compounds.[6] In contrast, the work with real lignin streams directly is tedious and leads to extensive analytical challenges including the structural determination of the starting material and the characterization of complex product mixtures.[2a,3a,7] Therefore, the synthesis of new, more advanced model compounds is highly desired and of general importance in this field.

Lignin contains different aromatic subunits (H, G, and S) and various types of linkages (Figure S1).[2a,3a,5] The occurrence of these linkages varies greatly depending on the plant type and pretreatment methods used. Thus, far, most studies have focused on the cleavage of the most abundant β-O-4 linkage using predominantly simple model compounds.[2a,3,6,8] Much less effort has been devoted to understanding the chemistry of other types of linkages such as β–β[9] and β-5[10] (Figure S2).[11]

It has become increasingly important to develop more sophisticated model compounds[12,13] that reflect the complexity of the native lignin structure. To the best of our knowledge, synthetic pathways to model compounds that combine multiple linkage types, contain all lignin-relevant functional groups, and at the same time are of limited molecular weight have not yet been developed. In this contribution, we provide scalable synthetic paths to access such advanced lignin model compounds and demonstrate their value in understanding the reactivity of the main linkages in real lignin feedstocks under depolymerization conditions.

The new class of advanced model compounds (**AB1**–**4**) are a combination of the β-O-4 and the β-5 linkage and contain phenolic and nonphenolic units (Figure 1). Variations on the

Received: April 29, 2016
Published: June 16, 2016

ACS Publications © 2016 American Chemical Society

DOI: 10.1021/jacs.6b04144
J. Am. Chem. Soc. 2016, 138, 8900–8911

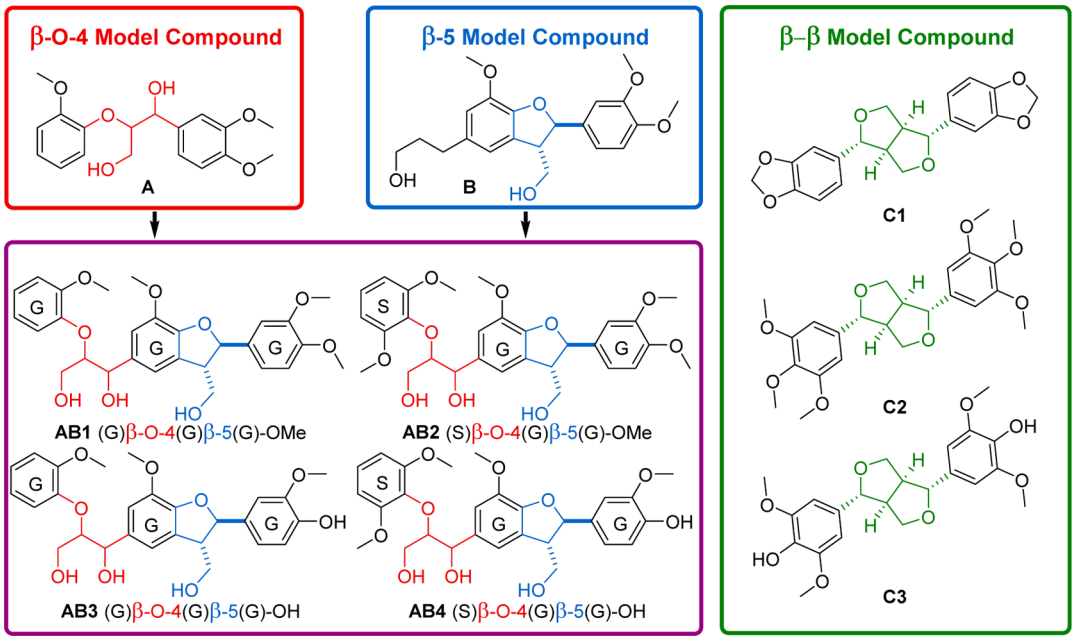

Figure 1. A summary of model compounds **A**, **B**, **C1−3** used during our catalytic studies, including novel *β*-O-4-*β*-5 dilinkage model compounds (**AB1−4**) synthesized in this work.

Scheme 1. Synthesis of Models AB1 and 2[a]

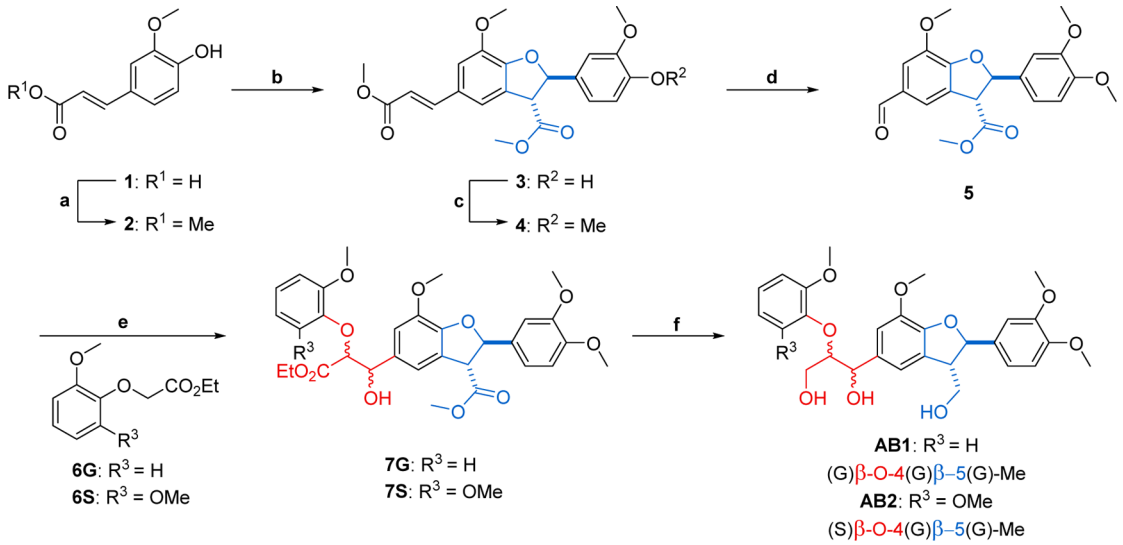

[a]Reagents and conditions: (a) TMSCl, MeOH, reflux, 1 h, 100%. (b) Ag_2O, DCM, 24 h, 39%. (c) MeI, K_2CO_3 acetone, reflux, 5 h, 66%. (d) $RuCl_3$ (0.1 mol %), $NaIO_4$, H_2SO_4, EtOAc/MeCN/H_2O (5:5:2), 0 °C, 3 h, 90%. (e) LDA, THF, −78 °C, 6 h, 82%* for **7G** and 80%* for **7S**. (f) $NaBH_4$/ MeOH, EtOH, 50 °C, 5 h, 90%* for **AB1** and 96%* for **AB2** (*combined yield of diastereomers).

β-O-4 side include guaiacyl (**AB1** and **AB3**) and syringyl (**AB2** and **AB4**) end groups. The *β*-5 moiety contains either a nonphenolic (**AB1** and **AB2**) or phenolic end group (**AB3** and **AB4**), whereby the methoxy simulates an internal *β*-5 linkage, whereas the phenolic group mimics a terminal *β*-5 linkage or the result of a cleaved *β*-O-4 linkage.

The reactivity of these model compounds (**AB1−4**) was subsequently evaluated in a catalytic method we have previously pioneered, which comprises acidolysis in conjunction with the stabilization of reactive intermediates under acetal formation conditions.[14] In addition to **AB1−4**, model compounds representing the *β*–*β* lignin linkage (**C1−3**) were selected for study. Furthermore, models **A**[15] and **B**[16] were selected for studying the isolated reactivity of the *β*-O-4 and *β*-5 linkages, respectively. Using a combination of these models (Figure 1), we were able to gain deeper understanding of the overall reactivity of lignin under these conditions. New reaction pathways and intermediates were established, and important products have been identified in actual lignin depolymerization mixtures.

RESULTS AND DISCUSSION

Synthesis of Novel (*β*-O-4)-(*β*-5) Lignin Model Compounds. To access the novel (*β*-O-4)-(*β*-5) models **AB1−4**, a divergent synthetic methodology was developed that allowed access to both nonphenolic (**AB1** and **AB2**) and phenolic (**AB3** and **AB4**) models (Schemes 1 and 2). Starting from commercially

DOI: 10.1021/jacs.6b04144
J. Am. Chem. Soc. 2016, 138, 8900−8911

Scheme 2. Synthesis of Phenolic Dilinkage Model Compounds AB3 and AB4[a]

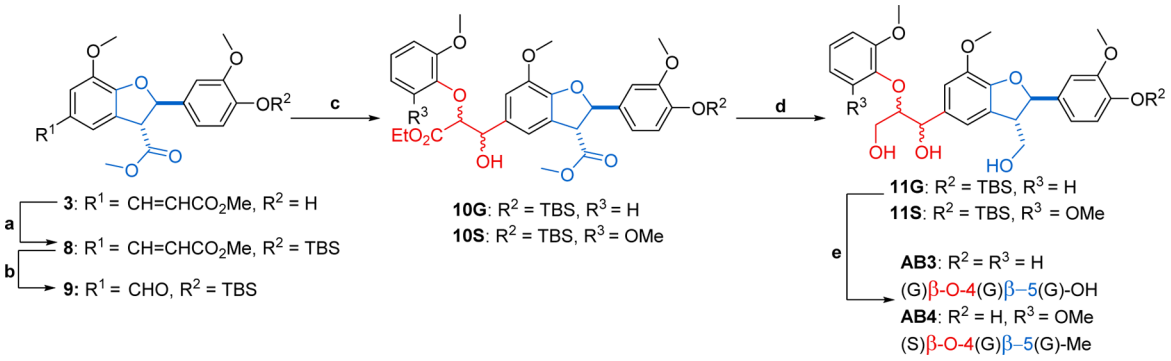

[a]Reagents and conditions: (a) TBSCl, imidazole, DMF, rt, 30 min, 89%. (b) $RuCl_3$ (0.1 mol %), $NaIO_4$, H_2SO_4, EtOAc/MeCN/H_2O (5:5:2), 0 °C, 6 h, 75%. (c) **6G** or **6S**, LDA, THF, −78 °C, 6 h, 80%* for **10G** and 85%* for **10S**. (d) $NaBH_4$/MeOH, EtOH, 50 °C, 5 h. (e) TBAF, THF, 5 min, 80%* for **AB3** and 83%* for **AB4** over 2 steps (*combined yield of diastereomers).

available ferulic acid (**1**) esterification with MeOH/TMSCl gave methyl ferulate (**2**), which when treated with silver(I) oxide underwent an oxidative dimerization to yield diferulate **3**.[17] This reaction is believed to proceed via a radical mechanism that is under thermodynamic control yielding the racemic *trans*-diferulate,[18] which possesses the same stereochemistry as the *β*-5 units in lignin.[19] Methylation of the phenol in **3** using CH_3I/K_2CO_3 gave **4** (Table S1),[20] and subsequent oxidative cleavage of the alkene in **4** using the $RuCl_3/NaIO_4$ system afforded aldehyde **5**. The relative stereochemistry of the *β*-5 motif in compounds **4** and **5** was confirmed by X-ray crystallography (Supporting Information section S4.2).

The *β*-O-4 moiety was installed by aldol reaction between **5** and **6G** to afford diester **7G** in 82% yield. In this unoptimized aldol protocol, a mixture of both the anti (erythro) and syn (threo) stereochemistry at the new stereogenic centers was formed in a 3:1 ratio[21] as determined by quantitative ^{1}H NMR analysis of the crude reaction mixture (Figure S3). Partial separation of the isomers could be achieved by column chromatography (Supporting Information section S4.1). However, in general, isomeric mixtures at the *β*-O-4 linkage (**A** and **AB1**−**4**) were prepared and used throughout this work for two main reasons: (i) In real lignin, the *β*-O-4 linkage is known to be present as a mixture of both anti and syn isomers.[19] (ii) In acid-mediated lignin degradation, the reaction proceeds via a common intermediate from both the anti or syn isomer.

Diastereomeric mixture **7G** was reduced using $NaBH_4$/MeOH in EtOH[22] to give **AB1** in 90% yield without separation of the anti and syn isomers. However, anti and syn diastereomers of **AB1** were obtained on a small scale from the separated isomers of precursor diester **7G** (Supporting Information section S4.1). Similarly, an aldol reaction between **5** and **6S** provided **7S** in 80% yield, which upon reduction gave the desired product **AB2** as a diastereomeric mixture in 96% yield.

To access phenolic model compounds **AB3** and **AB4**, a protecting group strategy was employed (Scheme 2). Protection of the phenolic group in **3** with TBSCl/imidazole afforded TBS-protected **8** in a quantitative yield with no need for further purification. From **8**, following an analogous synthetic route via **9** and **10G** or **10S** as outlined previously, TBS-protected models **11G** and **11S** were prepared and deprotected (TBAF) to give phenolic models **AB3** and **AB4** as mixtures of diastereomers in 80 and 83% yield, respectively, over the final two steps. With this set of novel models **AB1**−**4** in hand, we decided to study their reactivity in acid-mediated lignin depolymerization in the presence of ethylene glycol.

Reactivity of (*β*-O-4)-(*β*-5) Model Compounds under Acetal Formation Conditions. Acidolysis of lignin has received considerable attention due to the relevance of this method to the biorefinery concept. This approach was originally used to aid structural elucidation[11,23] and more recently for the production of well-defined aromatic compounds.[14,24] Using model compounds, two different reaction pathways (C2 and C3 pathways, Scheme 3) have been identified for the cleavage of the *β*-O-4 linkage and modification of the *β*-5 linkage.[24a,b,25] While the C3 pathway provides the Hibbert ketones, the C2 pathway yields C2-aldehydes upon release of formaldehyde, which can then undergo condensation reactions.[14,25,26] The balance of these pathways depends on the nature of the mineral acid used. With HBr, the C3 pathway dominates, whereas H_2SO_4 favors the C2 pathway.[26,27] Similar observations were made regarding the reactivity of the *β*-5 linkage. Lundquist et al. studied the reactivity of a *β*-5 model compound with different acids in mixtures of 1,4-dioxane/H_2O. While HBr gave mainly the C3-benzofuran product, triflic acid (HOTf) gave predominantly the C2-stilbene product.[28]

We have previously described the highly efficient cleavage of *β*-O-4 lignin model compounds using catalytic amounts of HOTf in conjunction with *in situ* stabilization of the resulting C2-aldehyde products as their ethylene glycol acetals.[14a] This concept was also extended to the depolymerization of lignin where recondensation reactions were markedly suppressed. However, important questions remained unanswered regarding the reactivity of the *β*−*β* and *β*-5 lignin linkages, and the products originating from these moieties were not identified. Furthermore, the released formaldehyde was neither detected nor quantified, and its role in recondensation was not clarified. The models **AB1**−**4** were ideally suited to answer these important questions.

*General Reactivity of (β-O-4)-(β-5) Models **AB1**−**4**.* First, the reactivity of **AB1**−**4** was examined under the reaction conditions we have previously established (HOTf/ethylene glycol).[14a] Full substrate conversion was seen within 15 min, resulting in the formation of guaiacol **G** (from **AB1** and **AB3**) or syringol **S** (from **AB2** and **AB4**) as determined by HPLC analysis (Scheme 4). These high yields of **G** and **S** were very similar to those found for simpler *β*-O-4 model compounds[14a] and demonstrated that the chemistry of the *β*-O-4 linkage was unaffected by the presence of the adjacent *β*-5 moiety.

DOI: 10.1021/jacs.6b04144
J. Am. Chem. Soc. 2016, 138, 8900−8911

Scheme 3. Known Pathways for the Acid-Mediated Cleavage of the Lignin β-O-4 Linkage and the Modification of the Lignin β-5 Linkage

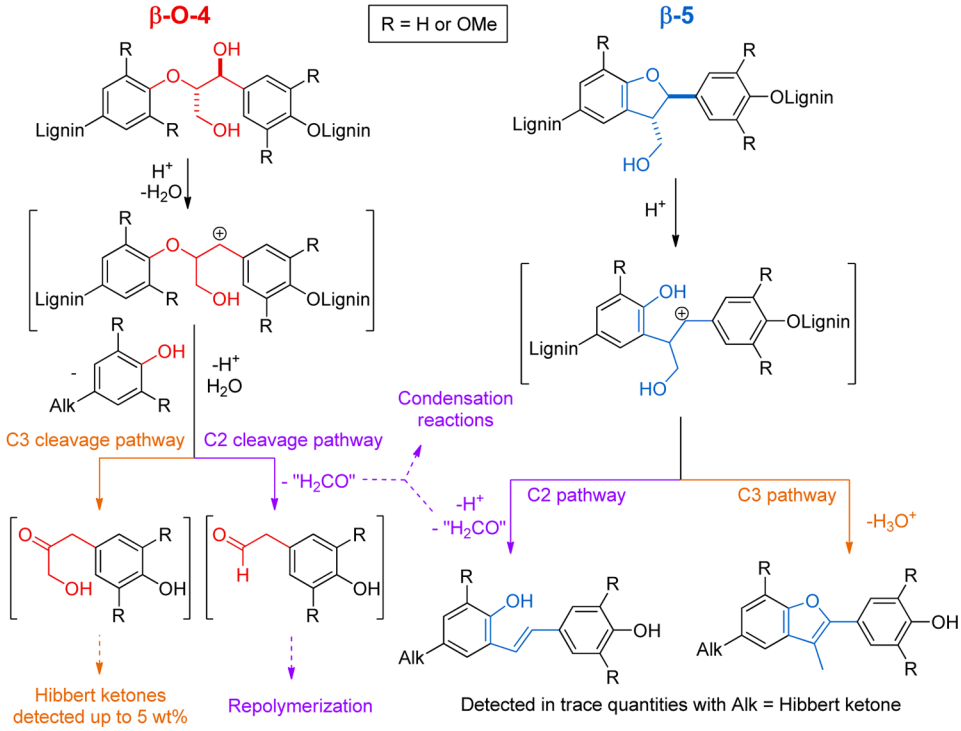

Scheme 4. Products Identified in Reactions of the (β-O-4)-(β-5) Model Compounds AB1−4[a]

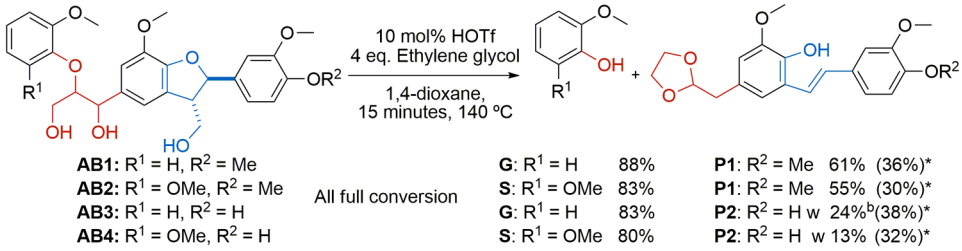

[a]See also Supporting Information sections S6.0 and S9.1. *Isolated yields from upscaled procedures with 5 mol % HOTf (Supporting Information section S11.0).

Depending on the substrate used (**AB1** and **AB2** or **AB3** and **AB4**), novel stilbene-acetals **P1** or **P2** were identified as the other major product (Scheme 4 and Supporting Information section S11.0). These products were likely formed by cleavage of the β-O-4 moiety in **AB1−4** to give the C2-aldehyde, which reacted with ethylene glycol (Scheme 3). Subsequent ring opening of the β-5 moiety then occurred also via the C2-pathway.[11b,28] **P1** and **P2** were isolated and fully characterized with the *E* stereochemistry being assigned on the basis of the coupling constants observed between the two alkene protons (16.5 and 16.4 Hz in **P1** and **P2**, respectively; Supporting Information section S11.0).[29]

In control reactions in the absence of ethylene glycol (Supporting Information section S9.2), the β-O-4 linkage was cleaved rapidly, and the guaiacol **G** yields were retained. However, a significant difference was seen in the reactivity of the remaining component of **AB1**, which formed a mixture of oligomeric products (according to GPC analysis, Supporting Information section S7.0). In contrast, GPC analysis of the reaction in the presence of ethylene glycol gave only the desired low molecular weight compounds. HPLC analysis also confirmed these observations (Figures S11 and S12) and similar results were obtained from **AB3** (Supporting Information sections S7.0 and S9.0).

*Product Formation Profiles and Reaction Intermediates Using (β-O-4)-(β-5) Model **AB1**.* To gain further insight, the acidolysis of **AB1** was studied in the presence of ethylene glycol and product formation profiles were recorded (Figure 2a and Supporting Information section S6.2). While **AB1** was consumed within 15 s, guaiacol **G** and acetal-stilbene **P1** were formed at a slower rate, reaching 79 and 56% yields, respectively. Two major signals were also observed by UPLC-MS analysis (both with $[M + H]^+$ = 465 g mol^{-1}) prior to the formation of **G** and **P1** (Figure 2a and Supporting Information section S10.1). These were attributed to the formation of isomeric alkenes **I1**, the products of dehydration and deformylation of **AB1**. While dehydration occurs by loss of the benzylic hydroxyl group in the β-O-4 unit,[25b,26b] deformylation could occur in the β-O-4 unit as well as the β-5 unit in **AB1**.

DOI: 10.1021/jacs.6b04144
J. Am. Chem. Soc. 2016, 138, 8900−8911

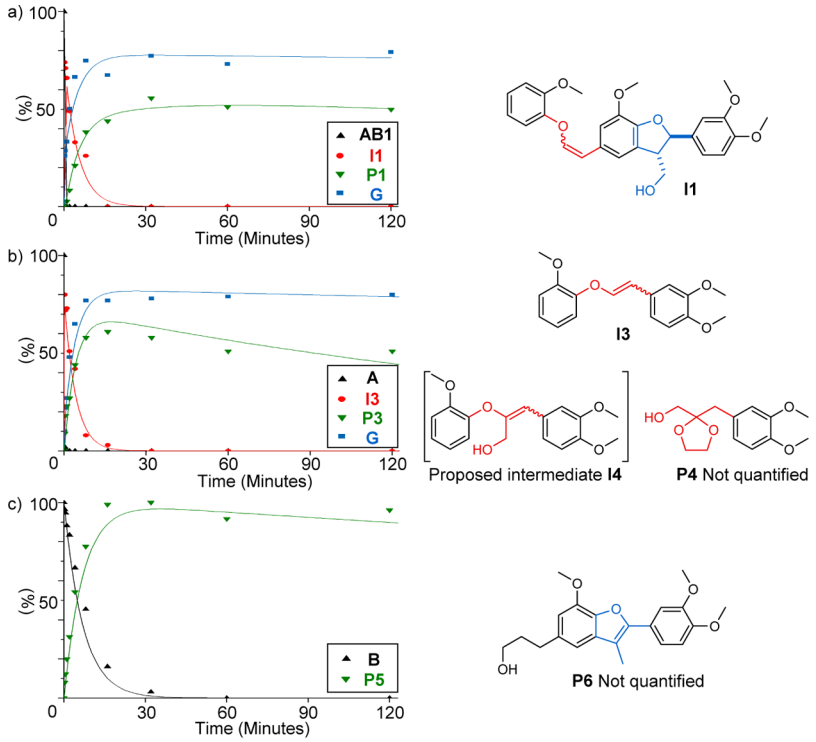

Figure 2. Reaction profiles using 5 mol % HOTf and 4 equiv of ethylene glycol at 140 °C in 1,4-dioxane with (a) (*β*-O-4)-(*β*-5) model compound **AB1**, (b) *β*-O-4 model compound **A**, and (c) *β*-5 model compound **B**. Dots show experimental data points, whereas the line is a modeled reaction profile (see also Supporting Information sections S6.2, S8 and S10).

Scheme 5. Reactions with HOTf and Ethylene Glycol with Model Compounds[a]

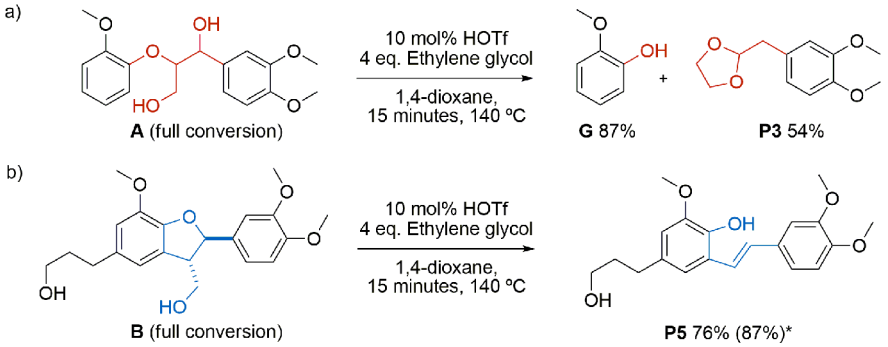

[a](a) *β*-O-4 Model compound **A** and (b) *β*-5 model compound **B**. *Isolated yield from upscaled procedures with 5 mol % HOTf (Supporting Information section S11.0)

Compounds **A**[15] and **B**[16] were used to investigate this issue further.

Study of the Relative Reactivity of β-O-4 and β-5 Units in ***AB1***. In a reaction with 10 mol % HOTf *β*-O-4, model **A** yielded 87% **G** and 54% acetal **P3** (Scheme 5a). Next, the reaction was monitored for 2 h (Figure 2b and Supporting Information sections S6.2 and S10.2).This revealed that **A** was rapidly consumed and that two main products were formed ($[M + H]^+$ = 287 g mol^{-1} by UPLC-MS). This reactivity pattern was analogous to that observed for **AB1**, and the detected mass of the products confirmed the formation of isomeric enol ethers **I3**, formed by acid-catalyzed dehydration/deformylation of the *β*-O-4 moiety en route to the C2-aldehyde. **I3** was further converted to **G** in 80% yield and **P3** in 61% yield.

When no ethylene glycol was added **G** was still obtained in good yield (69%), but the C2-aldehyde was not observed due to its conversion to a complex mixture of products, as seen for **AB1** under these conditions (Supporting Information section S9.0). During these reactions, ketal **P4**, the ethylene glycol ketal of the Hibbert ketone,[25a,30] was also identified (UPLC-MS, Supporting Information section S10.2). Its formation provided evidence for the functioning of the C3 cleavage pathway in these reactions. This pathway also leads to the formation of guaiacol **G**, so this explains the discrepancies between the yields of **G** and **P3** from **A** (and analogously the differences between the yields of **G** and **P1** formed from **AB1** above). Dehydrated intermediate **I4** (Figure 2b), the most likely precursor of **P4**, was previously observed when water was used as solvent but could not be detected under our reaction conditions.[24a,b]

Next, the reactivity of the *β*-5 model **B** was investigated. Upon reaction of **B** with 10 mol % HOTf and 4 equiv of ethylene

DOI: 10.1021/jacs.6b04144
J. Am. Chem. Soc. 2016, 138, 8900−8911

glycol, *E*-stilbene **P5** was obtained in 76% yield (Scheme 5b). However, the consumption of **B** was slow compared to those of **A** and **AB1**, and full conversion of **B** was only achieved after 30 min in contrast to 15 s for **A** and **AB1** (Figure 2c; Supporting Information section S6.2). The rates of formation of **P5** corresponded to the rates of **B** consumption, and no other reaction intermediates were identified. This is consistent with either the concerted deformylation/ring opening of **B** or the formation of short-lived intermediates en route to **P5** (*β*-5 C2 pathway shown in Scheme 3). Dehydrated benzofuran **P6** (Figure 2c) was identified as minor side product (UPLC-MS, Supporting Information section S10.3). **P6** originates from the C3-pathway previously identified on acid-catalyzed modification of the *β*-5 linkage (Scheme 3).[28]

*Proposed Reaction Pathways in Acidolysis of **AB1**.* Returning to the reactivity of **AB1** under acidolysis and acetal forming conditions, a series of reaction pathways were constructed (Scheme 6), and rate analysis provided the curve fits shown in the corresponding figures (on rate modeling, see Supporting Information section S8.0). The **AB1** acidolysis products ($[M + H]^+$ = 465 g mol^{-1}) were assigned to the *E* and *Z* isomers of enol ether **I1**, products of the reverse Prins reaction of **AB1** in which the *β*-5 linkage remains unmodified. This is consistent with the very fast formation of **I3** from **A**. The subsequent cleavage of **I1** to form **G** and an elusive intermediate **I1a** (calculated rate of consumption **I1** = 0.35 min^{-1} vs **I3** = 0.22 min^{-1}) is the subsequent step followed by the modification of the *β*-5 linkage via C2 pathway to give the final acetal stilbene product **P1** (rate of formation = 0.14 min^{-1} for both **P1** and **P5**). The C3 pathway for the *β*-5 modification also occurs as a minor side reaction providing traces of **P8** similar to the traces of **P6** formed from **B**. The second existing route by which **G** is formed from **AB1** is the C3 pathway analogous to that identified using the *β*-O-4 model compound **A**. This route leads to **P7** ($[M + H]^+$ = 403 g mol^{-1}), the corresponding Hibbert ketal analogue (Supporting Information section S10.1). For the *β*-O-4 cleavage, the C2 pathway is dominant over the C3 pathway under these reaction conditions (a 3:1 ratio based on the modeled rates and the **P1** to **G** yield discrepancy). The modification of the *β*-5 linkage occurs nearly exclusively via the C2 pathway.

Determination and Quantification of the Formaldehyde Released from the (*β*-O-4)-(*β*-5) Models. During the acidolysis of models **AB1**, **A**, and **B**, the C2 reaction pathways for both the *β*-5 and *β*-O-4 linkages involve the formal loss of a carbinol group. Although previous studies agree that this is achieved through the release of formaldehyde,[24b,25] there has been little direct evidence to support this or attempts to quantify the amount of formaldehyde released, likely due to experimental difficulties. Our unique reaction conditions, however, allow for identification and quantification of the released formaldehyde trapped as its ethylene glycol acetal, 1,3-dioxolane **Z** (Scheme 7).

Scheme 7. 1,3-Dioxolane Z Formation from the Reactions of A, B, or AB1 with HOTf and Ethylene Glycol

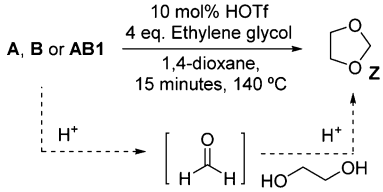

Reactions of **AB1**, **A**, and **B** were repeated in d_8-1,4-dioxane. In all cases, the corresponding 1,3-dioxolane **Z** was clearly identified (signals at *δ* 4.77 and *δ* 3.76 in ^{1}H NMR spectra), and the amounts of **Z** as well as acetal products **P1** and **P3** were quantified using an internal standard (Figure 3, for details see Supporting Information section S12). In the case of **A**, a 56% yield of **Z** was observed and this matched well with the 66% yield of C2-acetal **P3** found in the same sample (Figure 3a and Supporting Information section S12.1). Also, for the *β*-5 model **B**, the amount of **Z** (81% yield) was consistent with that of the

Scheme 6. Overview of the Detected Reaction Sequences from the HOTf-Catalyzed Cleavage and Modification of AB1 in 1,4-Dioxane at 140 °C

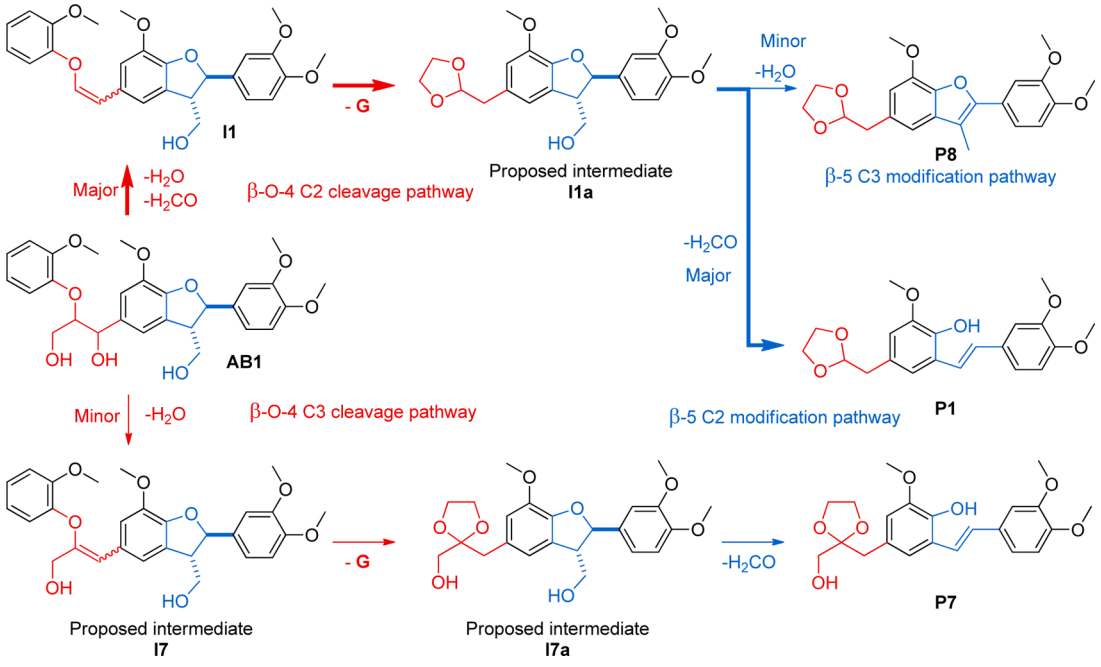

DOI: 10.1021/jacs.6b04144
J. Am. Chem. Soc. 2016, 138, 8900−8911

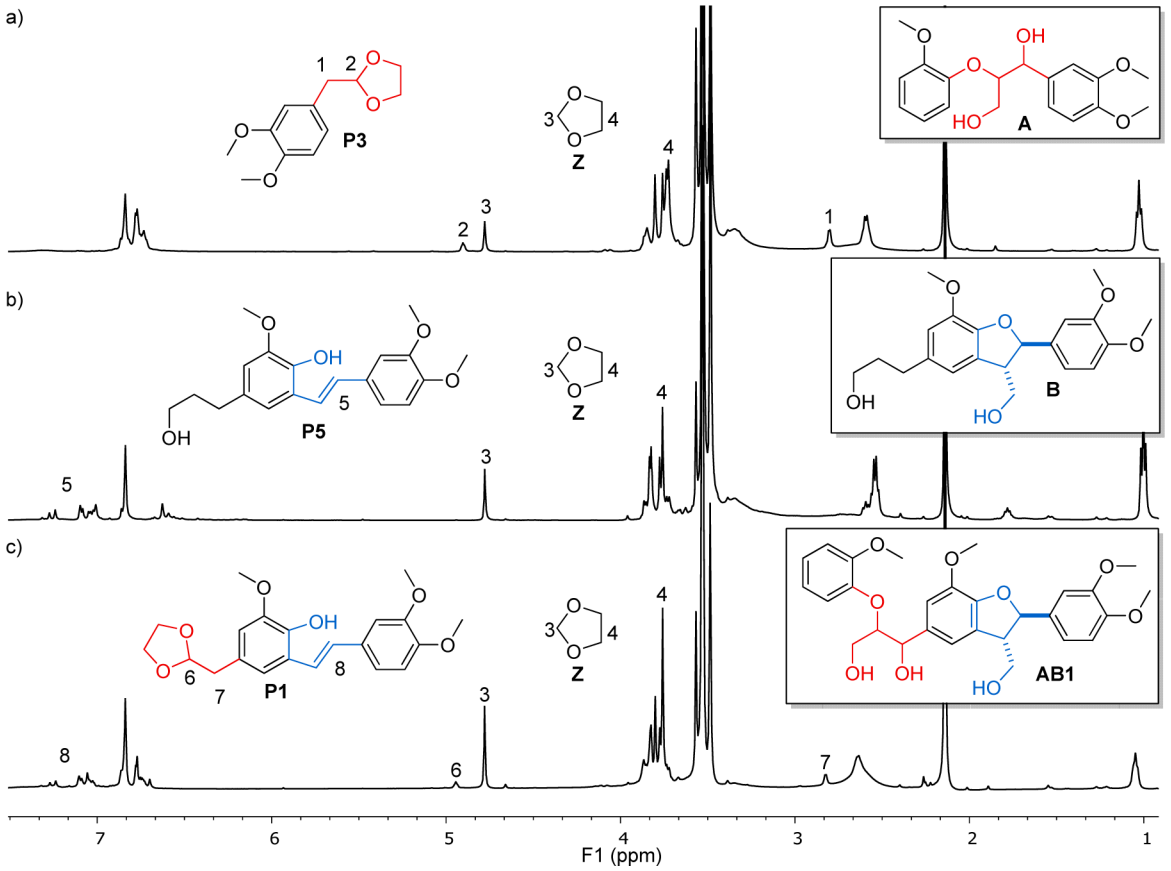

Figure 3. Crude ^{1}H NMR spectra of the reactions of (a) **A**, (b) **B**, and (c) **AB1**. Reaction conditions: 10 mol % HOTf, 4 equiv ethylene glycol, 1,4-dioxane-d_8, 140 °C, 15 min, and 1,2,4,5-tetramethylbenzene as internal standard.

Scheme 8. Epimerization of β–β Model C1a under Acid Conditions[a]

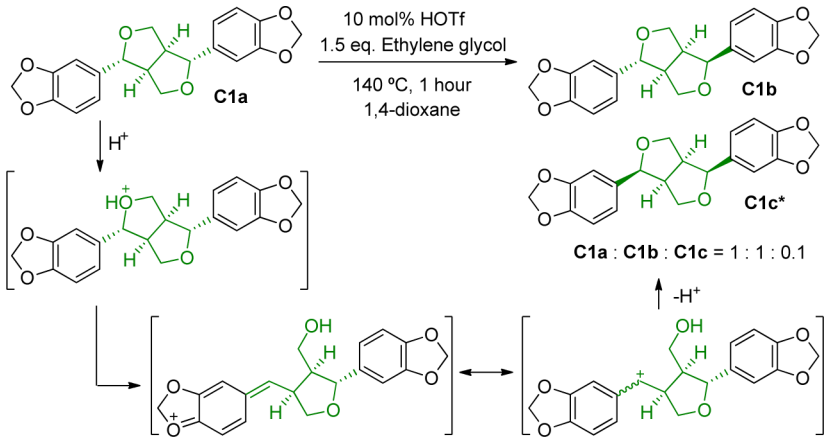

[a]*: Via a second epimerization reaction at the other benzylic position

corresponding C2 product, **P5** (76% yield by HPLC from a separate reaction, Figure 3b and Supporting Information section S12.2). Finally, for **AB1** an 85% yield of **Z** based on the release of 2 equiv of formaldehyde was found (Figure 3c and Supporting Information section S12.3). The amount of **P1** was slightly lower than expected based on the yield of **Z** (62% **P1** vs 85% **Z**), but is consistent with the HPLC yields discussed above (Scheme 4) combined with the observation that the C3 pathway for the cleavage of the β-O-4 linkage still leads to a product in which the β-5 unit has been modified according to the C2 pathway leading to additional **Z** (Scheme 6). The observed quantities of **Z**, together with the identified products of the complementary C2 pathways, are strong indications that most of the released formaldehyde is trapped as its corresponding acetal. Formaldehyde has been previously implicated in condensation reactions;[14a,31] thus, the use of ethylene glycol in our catalytic system contributes to eliminating the adverse effects of formaldehyde. This, together with the trapping of other reactive intermediates (aldehydes), explains the success of this methodology when applied to lignin.[14a]

Examination of the Reactivity of β–β Model Compounds. The effect of our standard acidolysis conditions on

DOI: 10.1021/jacs.6b04144
J. Am. Chem. Soc. 2016, 138, 8900–8911

Scheme 9. Schematic Showing of Specific Linkages as They Would Appear in Lignin and Expected Cleavage Products[a]

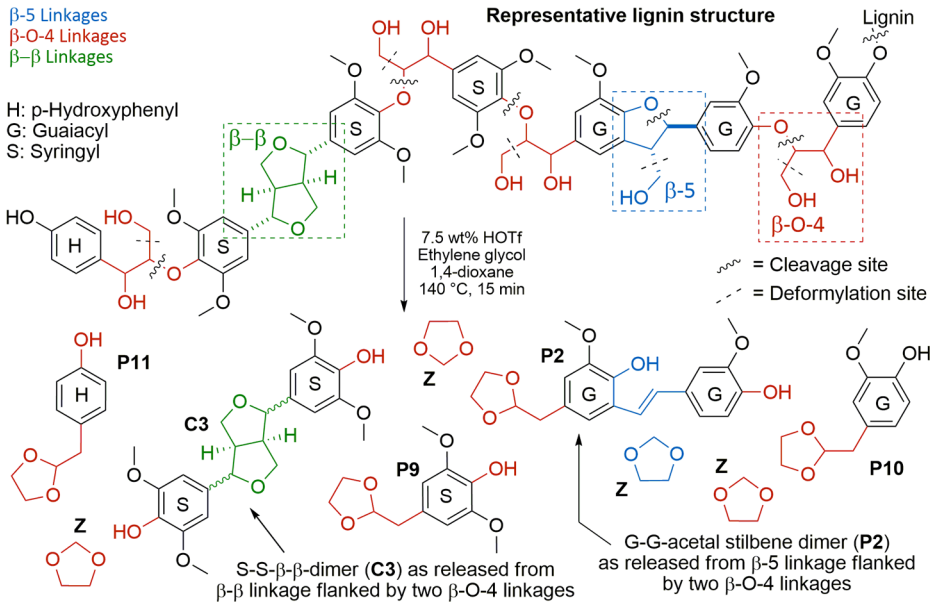

[a]A hypothetic lignin structure is shown containing *β*-O-4, *β*-5 and *β*–*β* linkages.

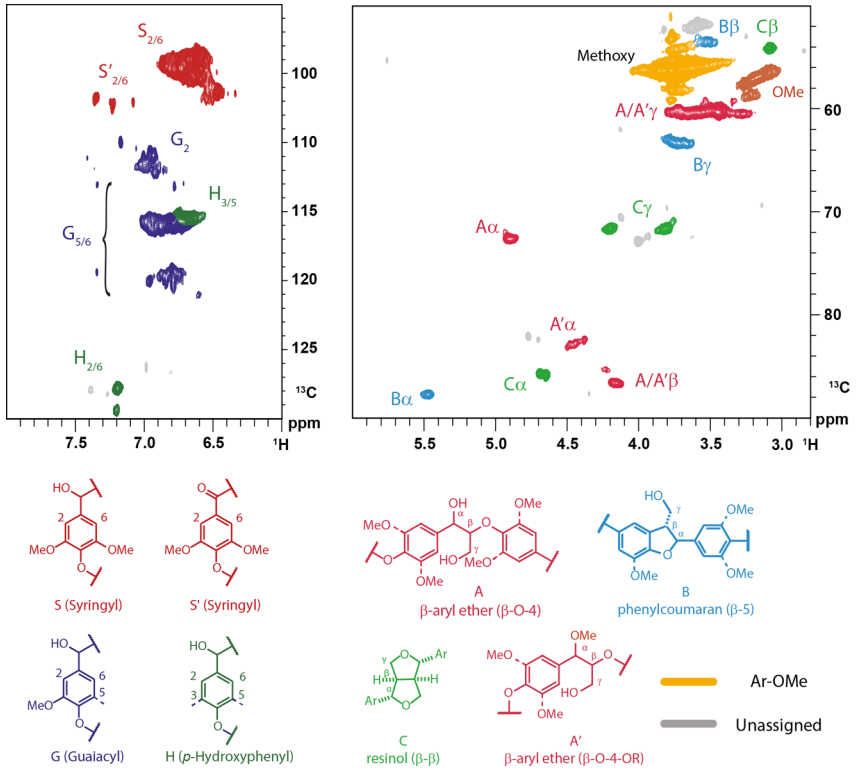

Figure 4. 2D HSQC NMR spectrum of walnut methanosolv lignin showing areas used for the quantification of visible linkages and determination of S/G/H ratios.

the *β*–*β* motif was studied using the model **C1a** (sesamin, Scheme 8) because **C1a** has the same relative configuration as the *β*–*β* linkage in lignin.[5,9a] Acidolysis of **C1a** led to a remarkably clean reaction (Supporting Information section S13.1) with the main products being epimers **C1b** (asarinin/episesamin) and **C1c** (epiasarinin/diasesamin, Scheme 8).[9b,32] The ratio of **C1a**/**C1b**/**C1c** was 1:1:0.1 (^{1}H NMR, Figure S19) with a >95% mass balance (GC-FID) being observed. Reaction of **C1a** in the absence of ethylene glycol provided the same product mixture indicating little influence of the diol on this reaction (Figure S20). The same product distribution was also observed when **C2a** (yangambin) was reacted under these conditions (Figure S21). Epimerization reactions for similar compounds have been previously reported using different Lewis acids.[9a,b,32] Phenolic versions of these compounds (e.g., pinoresinol and syringaresinol **C3**, Figure 1) and their epimers were previously obtained during lignin

DOI: 10.1021/jacs.6b04144
J. Am. Chem. Soc. 2016, 138, 8900–8911

acidolysis[11c,23a,26a] and were again identified in this work (*vide infra*). These results indicate no effect of ethylene glycol on the products formed via acidolysis of the $\beta-\beta$ motif in lignin.

Identification of Dimeric Products in Lignin-Derived Product Mixtures. This work culminated in our analysis of lignin-derived product mixtures to assess if the reactions observed in the model compounds translated to the natural material itself. A typical organosolv lignin consists predominantly of the most abundant β-O-4 linkage and the less abundant (about 10%) β-5 and $\beta-\beta$ linkages (other minor linkages were not considered).[5] Therefore, it is very likely that the β-5 linkages will be flanked by β-O-4 linkages, a situation that inspired the design of **AB1−4**. The same will hold true for the $\beta-\beta$ linkages. Exposure of lignin to our catalytic acidolysis conditions would therefore be expected to give phenolic acetals **P9−11** as the major products via the C2-pathways because they result from the cleavage of neighboring β-O-4 linkages (Scheme 9)[14a] as well as small amounts of Hibbert ketals via the C3 pathway. A β-5 dimer flanked by two β-O-4 linkages should result in stilbene compounds such as **P2** via the C2 β-O-4 cleavage pathway plus smaller amounts of ketal structures such as **P7** (Scheme 6) through the C3 β-O-4 cleavage pathway. A $\beta-\beta$ dimer flanked by two β-O-4 linkages should give epimerized diphenolic $\beta-\beta$ fragments like **C3** (Scheme 9).[11c,23a]

To confirm this, catalytic depolymerization reactions were carried out using pine, beech, and walnut shell organosolv lignins. These lignins were obtained by standard organosolv processing and characterized using 2D HSQC NMR (Figure 4) and GPC for which the most relevant data are summarized in Table 1 (Isolation and characterization details in Supporting Information sections S14.0 and S15.0).

Next, 50 mg samples of these lignins were subjected to the catalytic acidolysis conditions. The crude reaction mixtures were processed by extraction to obtain LMW and high molecular weight fractions (Supporting Information sections S16.0 and S17.0). The LMW fractions were analyzed by GC-FID and GC-MS, and the expected main product acetals (**P9−11**, Scheme 9) were quantified using an internal standard (Table 2). The **P9** versus **P10** ratios corresponded well to the amount of **S, G** and **H** units in the lignin starting material. Moreover, the total acetal yields for the respective lignins were dependent on the number of β-O-4 linkages in the original lignin (compare Tables 1 and 2). In the case of ethanosolv beech lignin, the β-O-4 moiety showed increased ethanol incorporation as a result of the organosolv procedure.[33] This is a likely explanation of the slightly higher than expected acetal yields based on the overall β-O-4 content determined by NMR. All acetal yields corresponded well to the isolated yields that we have previously reported (Supporting Information section S17.0 for analysis details).[14a] In these reactions, small amounts of products were also seen that correlate to cleavage of the β-O-4 moiety via the C3-pathway, including **P12** (Figure 5a).

Table 2. Product Distribution P9−P11 Obtained from Lignin Acidolysis Reaction Using HOTf and in the Presence of Ethylene Glycol[a]

entry	lignin	**P9** (wt %)[b]	**P10** (wt %)[b]	**P11** (wt %)	total **P9−11** (wt %)
1	pine methanosolv		4.4	0.1	4.5
2	beech ethanosolv	4.8	2.6		7.4
3	walnut methanosolv	7.0	3.9	0.4	11.3

[a]Conditions: 50 mg of lignin, 60 mg of ethylene glycol, 7.5 wt % HOTf, 1 mL of 1,4-dioxane, 30 min, 140 °C, in sealed pressure vessel, *n*-octadecane as GC internal standard. LMW fraction was obtained by extraction of dried reaction solid with 9:1 toluene/DCM. [b]Determined by GC-FID referring to the amount of starting lignin, structures shown in Scheme 9.

The product mixtures from pine lignin were investigated first. Gratifyingly, acetal stilbene **P2** could be identified by GC-MS analysis and its presence verified by spiking with an authentic sample of **P2** (Figure 5a and Table S8). The yield of **P2** was determined as 2 wt %, in agreement with the relatively high percentage of β-5 linkages (10 per 100 aromatic units) in this lignin. Because pine lignin contains only **G** units, none of the corresponding **S** containing acetal stilbenes were observed. Compound **P13** (analogous to **P8**) was also detected (Figure 5a). No $\beta-\beta$ dimer fragments were identified in this reaction mixture given the limited amount of such linkages present in this lignin (<1 $\beta-\beta$ linkages per 100 aromatic units, Table 1).

The beech organosolv and the walnut shell methanosolv lignins were richer in $\beta-\beta$ linkages (4 and 8 $\beta-\beta$ linkages per 100 aromatic units respectively); thus, $\beta-\beta$-containing fragments derived from these lignins were successfully identified. The presence of syringaresinol **C3a** was verified by spiking with an authentic sample for both lignins (Figures 5b and S29). **C3a** and epimer **C3b** were found as a 1:1 mixture and identified based on their identical molecular weight and fragmentation patterns. The observation of **C3**, a $\beta-\beta$ dimer of two **S** units, is consistent with the relatively high amount of **S** units in these lignins. In addition, it is known that **S** units are more likely to undergo $\beta-\beta$ dimer formation during lignin biosynthesis.[34] The combined yields of these epimers from beech and walnut lignin were 2.6 and 5.5 wt %, respectively, in line with the amount of the respective linkages in these lignins (GC-MS analysis see Tables S9 and S10). Additionally, in the samples obtained from the walnut methanosolv lignin, trace quantities of **P2** and **P13** were observed.

The above results clearly demonstrate that the chemistry established using (β-O-4)-(β-5) model compounds **AB1−4** as

Table 1. Lignin Characteristics Determined by GPC and 2D-HSQC Analysis

				linkages (per 100 C_9 units)[c]			
entry	lignin	M_n (Da), M_w (Da), Đ[a]	**S, G, H** (%)[b]	β-O-4[d]	β-O-4-OR[e]	β-5	$\beta-\beta$
1	pine methanosolv	1075, 2088, 1.9	0, 100, trace	11	5	10	1
2	beech ethanosolv	928, 2016, 2.2	68, 32, 0	7	4	3	4
3	walnut methanosolv	808, 1518, 2.2	65, 29, 6	26	12	7	8

[a]Determined by GPC (THF) against polystyrene standards (Supporting Information section S15.1). [b]Determined by 2D-HSQC using volume integrals for the corresponding aromatic protons corrected for the amount of protons (Supporting Information section S15.2). [c]Determined by 2D-HSQC by comparing the volume integrals for the aromatic protons to the volume integrals of the benzylic protons of the linkages corrected for the amount of protons (Supporting Information section S15.2). [d]Total number of β-O-4 linkages (i.e. α-OH + α-OR). [e]Amount of α-methoxylated/ethoxylated units.

DOI: 10.1021/jacs.6b04144
J. Am. Chem. Soc. 2016, 138, 8900−8911

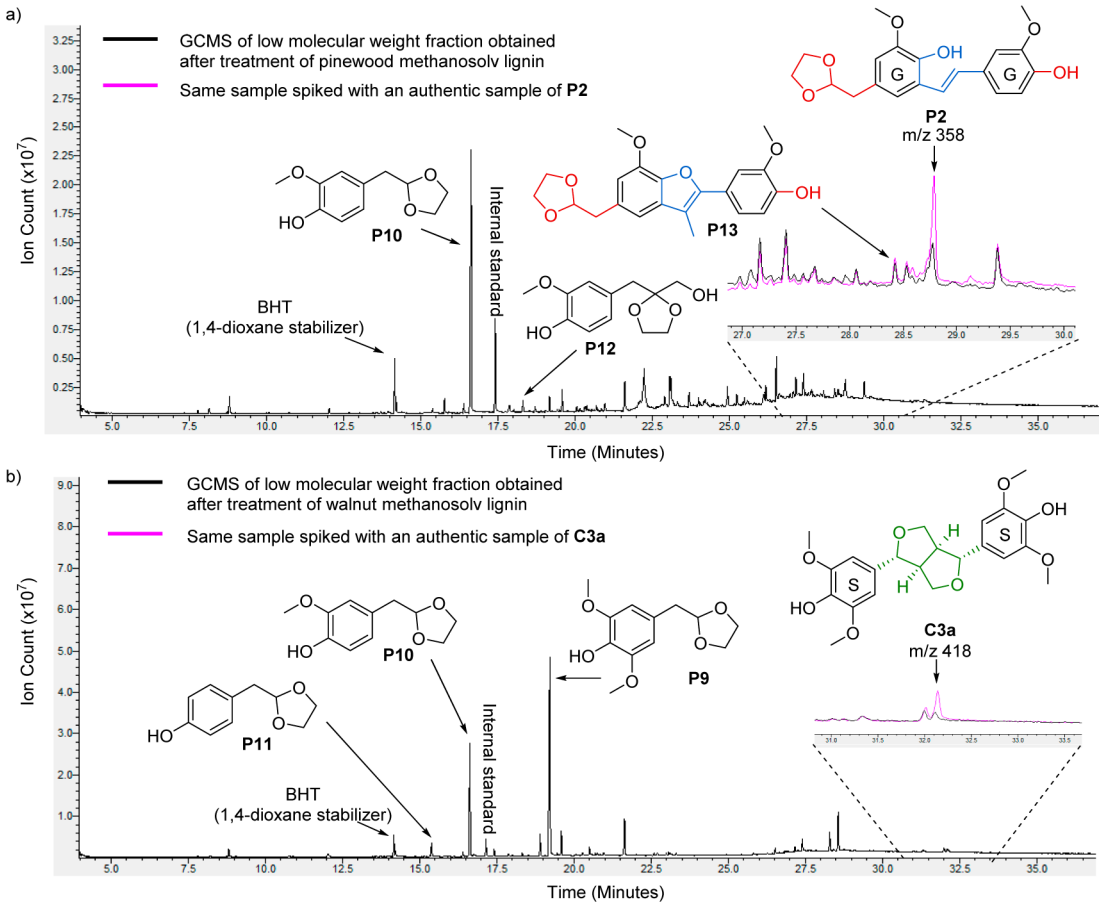

Figure 5. GC-MS traces of product mixtures obtained from the depolymerization of (a) methanosolv pine lignin and the same sample spiked with an authentic sample of compound **P2** and (b) beech wood ethanosolv lignin and the same sample spiked with an authentic sample of compound **C3a**. Reaction conditions: 50 mg of lignin, 60 mg of ethylene glycol, 7.5 wt % HOTf, 1 mL of 1,4-dioxane, 30 min, 140 °C, in sealed pressure vessel, *n*-octadecane as GC internal standard (For more detailed analysis of the GC-MS trace, see Supporting Information section S17.2).

well as $\beta-\beta$ model compounds **C1** and **C2** using acetal formation conditions can be directly extrapolated to the depolymerization of lignin under the same conditions. The unambiguous identification of structurally diverse dimeric compounds such as **P2** or **C3** in complex lignin-derived product mixtures would prove extremely challenging solely based on GC-MS or UPLC-MS analysis. With lignin-relevant model compounds such as **AB1−4**, however, the formation of these compounds can be rationalized. Analysis of the product mixtures also confirmed the dominance of the C2 reaction pathways, which should coincide with formaldehyde release from the β-O-4 and β-5 motifs. A separate set of experiments was conducted to confirm this using beech ethanosolv and walnut methanosolv lignin in d_8-1,4-dioxane. The ^{1}H NMR analysis of these reactions revealed the formation of 1,3-dioxolane **Z** (Figure 6 and Supporting Information section S18.0). The yields of **Z** from beech and walnut lignin were 1 and 4.2 wt %, respectively (quantified using an internal standard). This corresponds to the amounts of acetals **P9−P11** detected. It is remarkable that the reactivity trends established using our new models **AB1−4** were also in good agreement in terms of formaldehyde release with the results obtained with actual lignin samples. A further advantage of trapping the released formaldehyde is that it leads to a more complete overall carbon mass balance of the lignin depolymerization reaction. The high yield of 1,3-dioxolane **Z** bodes well for the large-scale production of this compound from lignin, in addition to the valuable aromatics, because 1,3-dioxolane **Z** already finds use as a solvent.

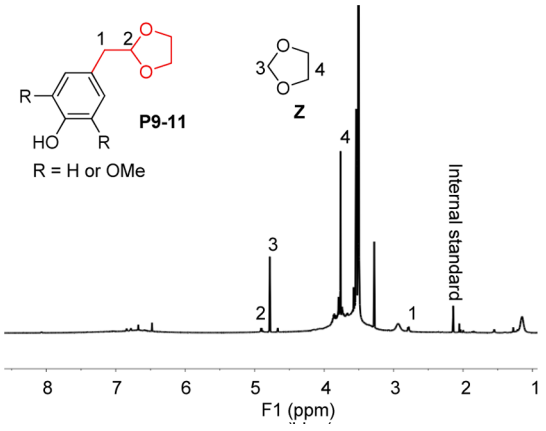

Figure 6. ^{1}H NMR spectrum of the crude reaction mixture obtained from the depolymerization of 50 mg of walnut methanosolv lignin demonstrating the formation of 1,3-dioxolane **Z**. Reaction conditions: 7.5 wt % HOTf, 60 mg of ethylene glycol at 140 °C for 30 min, quenched by the addition of 5 μL Et_3N.

CONCLUSIONS

We have described the synthesis of a new class of (β-O-4)-(β-5) lignin models **AB1−4** that are realistic representations of an abundant lignin fragment (particularly in softwoods). These models allowed for in-depth catalysis studies and enabled a detailed understanding of the controlled catalytic depolymeriza-

DOI: 10.1021/jacs.6b04144
J. Am. Chem. Soc. 2016, 138, 8900−8911

tion of lignin itself. This was possible because **AB1−4** are sufficiently complex to mimic lignin reactivity but still enable product analysis. We also gained detailed insight into the acid-catalyzed cleavage of **AB1−4** as well as other β-O-4, β-5 and $\beta-\beta$ model compounds. It was demonstrated that the mild depolymerization strategies presented herein were highly efficient in the cleavage of C−O bonds, whereas the main C−C linkages in the β-5 and $\beta-\beta$ were left intact, with the only C−C bond scission being the release of formaldehyde. Therefore, to obtain high yields of aromatic monomers, lignins with high β-O-4 content are desired. The structure and quantity of dimeric products, however, relates to the type and number of C−C bonds present in the starting lignin structure. Major reaction pathways (C2 and C3, Schemes 3 and 6) and important intermediates were identified. In addition, novel dimeric products, such as *E*-acetal stilbenes **P1** and **P2** were isolated. This has, for the first time, allowed the identification of these products in depolymerization mixtures generated from pine and walnut lignins.

Recently, Sels and co-workers found the use of ethylene glycol beneficial in reductive lignin depolymerization.[35] Our previous studies also addressed the advantages of using ethylene glycol under acidolysis conditions.[14] Herein, we further specified the benefits of using ethylene glycol in our reactions. First, ethylene glycol stabilizes the various C2-aldehydes formed on cleavage of the β-O-4 linkages. Further, ethylene glycol plays a role in "trapping" the formaldehyde released both from the β-O-4 as well as the β-5 linkage. Importantly, we were able to quantify the amount of released formaldehyde in model and lignin reactions via the corresponding 1,3-dioxolane **Z** formed.

Overall, a close correlation between the reactivity of **AB1−4** and lignin was found. Thus, our novel (β-O-4)-(β-5) lignin models should find general use in future catalytic lignin depolymerization studies and will enable further improvements in our understanding of the reactivity of lignin. This is an essential component of establishing financially viable biorefineries.

■ ASSOCIATED CONTENT

Supporting Information

The Supporting Information is available free of charge on the ACS Publications website at DOI: 10.1021/jacs.6b04144.

Synthetic procedures and analytical data for described model compounds; procedures and analytical data for reactions with model compounds as well as product isolation and characterization; lignin isolation procedures and characterization; lignin depolymerization procedures; analytical data for product mixtures (PDF)

Crystallographic data for compounds **4** and **5** (CIF)

■ AUTHOR INFORMATION

Corresponding Authors

*E-mail: njw3@st-andrews.ac.uk.

*E-mail: k.barta@rug.nl.

Author Contributions

C.W.L. and P.J.D. contributed equally to this work.

Notes

The authors declare no competing financial interest.

■ ACKNOWLEDGMENTS

This work was funded by the EP/J018139/1, EP/K00445X/1 grants (N.J.W. and P.C.J.K.), an EPSRC Doctoral Prize Fellowship (C.S.L.), and the European Union (Marie Curie ITN "SuBiCat" PITN-GA-2013-607044, C.W.L., N.J.W., P.C.J.K., P.J.D., K.B., J.G.V.). We acknowledge the EPSRC UK National Mass Spectrometry Facility at Swansea University for mass spectrometry analysis.

■ REFERENCES

(1) (a) Tuck, C. O.; Pérez, E.; Horváth, L. T.; Sheldon, R. A.; Poliakoff, M. *Science* **2012**, *337*, 695−699. (b) Ragauskas, A. J.; Beckham, G. T.; Biddy, M. J.; Chandra, R.; Chen, F.; Davis, M. F.; Davison, B. H.; Dixon, R. A.; Gilna, P.; Keller, M.; Langan, P.; Naskar, A. K.; Saddler, J. N.; Tschaplinski, T. J.; Tuskan, G. A.; Wyman, C. E. *Science* **2014**, *344*, 1246843.

(2) (a) Zakzeski, J.; Bruijnincx, P. C. A.; Jongerius, A. L.; Weckhuysen, B. M. *Chem. Rev.* **2010**, *110*, 3552−3599. (b) Vennestrøm, P. N. R.; Osmundsen, C. M.; Christensen, C. H.; Taarning, E. *Angew. Chem., Int. Ed.* **2011**, *50*, 10502−10509.

(3) (a) Xu, C.; Arancon, R. A. D.; Labidi, J.; Luque, R. *Chem. Soc. Rev.* **2014**, *43*, 7485−7500. (b) Zaheer, M.; Kempe, R. *ACS Catal.* **2015**, *5*, 1675−1684. (c) Kärkäs, M. D.; Matsuura, B. S.; Monos, T. M.; Magallanes, G.; Stephenson, C. R. *Org. Biomol. Chem.* **2016**, *14*, 1853−1914.

(4) Selected novel approaches for lignin depolymerization: (a) Rahimi, A.; Ulbrich, A.; Coon, J. J.; Stahl, S. S. *Nature* **2014**, *515*, 249−252. (b) Parsell, T. H.; Owen, B. C.; Klein, I.; Jarrell, T. M.; Marcum, C. L.; Haupert, L. J.; Amundson, L. M.; Kenttämaa, H. I.; Ribeiro, F.; Miller, J. T.; Abu-Omar, M. M. *Chem. Sci.* **2013**, *4*, 806−813. (c) Hanson, S. K.; Baker, R. T. *Acc. Chem. Res.* **2015**, *48*, 2037−2048. (d) Feghali, E.; Carrot, G.; Thuéry, P.; Genre, C.; Cantat, T. *Energy Environ. Sci.* **2015**, *8*, 2734−2743. (e) Lancefield, C. S.; Ojo, O. S.; Tran, F.; Westwood, N. J. *Angew. Chem., Int. Ed.* **2015**, *54*, 258−262. (f) Klein, I.; Marcum, Ch.; Kenttamaa, H.; Abu-Omar, M. M. *Green Chem.* **2016**, *18*, 2399−2405. (g) Van den Bosch, S.; Schutyser, W.; Vanholme, R.; Driessen, T.; Koelewijn, S.-F.; Renders, T.; De Meester, B.; Huijgen, W. J. J.; Dehaen, W.; Courtin, C. M.; Lagrain, B.; Boerjan, W.; Sels, B. F. *Energy Environ. Sci.* **2015**, *8*, 1748−1763.

(5) (a) Boerjan, W.; Ralph, J.; Baucher, M. *Annu. Rev. Plant Biol.* **2003**, *54*, 519−546. (b) Ralph, J.; Lundquist, K.; Brunow, G.; Lu, F.; Kim, H.; Schatz, P. F.; Marita, J. M.; Hatfield, R. D.; Ralph, S. A.; Christensen, J. H.; Boerjan, W. *Phytochem. Rev.* **2004**, *3*, 29−60.

(6) A comprehensive review: Deuss, P. J.; Barta, K. *Coord. Chem. Rev.* **2016**, *306*, 510−532.

(7) (a) Barta, K.; Ford, P. C. *Acc. Chem. Res.* **2014**, *47*, 1503−1512. (b) Dutta, S.; Wu, K. C.-W.; Saha, B. *Catal. Sci. Technol.* **2014**, *4*, 3785−3799.

(8) Selected examples: (a) Nichols, J. M.; Bishop, L. M.; Bergman, R. G.; Ellman, J. A. *J. Am. Chem. Soc.* **2010**, *132*, 12554−12555. (b) Wu, A.; Patrick, B. O.; Chung, E.; James, B. R. *Dalton Trans.* **2012**, *41*, 11093−11106. (c) Steves, J. E.; Stahl, S. S. *J. Am. Chem. Soc.* **2013**, *135*, 15742−15745. (d) Nguyen, J. D.; Matsuura, B. S.; Stephenson, C. R. J. *J. Am. Chem. Soc.* **2014**, *136*, 1218−1221. (e) Feghali, E.; Cantat, T. *Chem. Commun.* **2014**, *50*, 862−865. (f) vom Stein, T.; den Hartog, T.; Buendia, J.; Stoychev, S.; Mottweiler, J.; Bolm, C.; Klankermayer, J.; Leitner, W. *Angew. Chem., Int. Ed.* **2015**, *54*, 5859−5863. (g) Dabral, S.; Mottweiler, J.; Rinesch, T.; Bolm, C. *Green Chem.* **2015**, *17*, 4908−4912.

(9) (a) Tran, F.; Lancefield, C. S.; Kamer, P. C. J.; Lebl, T.; Westwood, N. J. *Green Chem.* **2015**, *17*, 244−249. (b) Aldous, D. J.; Dalençon, A. J.; Steel, P. G. *Org. Lett.* **2002**, *4*, 1159−1162. (c) Das, B.; Madhusudhan, P.; Venkataiah, B. *Synth. Commun.* **2000**, *30*, 4001−4006.

(10) (a) Macala, G. S.; Matson, T. D.; Johnson, C. L.; Lewis, R. S.; Iretskii, A. V.; Ford, P. C. *ChemSusChem* **2009**, *2*, 215−217. (b) Atesin, A. C.; Ray, N. A.; Stair, P. C.; Marks, T. J. *J. Am. Chem. Soc.* **2012**, *134*, 14682−14685. (c) Shimada, M.; Habe, T.; Higuchi, T.; Okamoto, T.; Panijpan, B. *Holzforschung* **1987**, *41*, 277−285. (d) Elegir, G.; Daina, S.; Zoia, L.; Bestetti, G.; Orlandi, M. *Enzyme Microb. Technol.* **2005**, *37*, 340−346. (e) Canevali, C.; Orlandi, M.; Pardi, L.; Rindone, B.; Scotti, R.; Sipila, J.; Morazzoni, F. *J. Chem. Soc., Dalton Trans.* **2002**, 3007−3014. (f) Cui, F.; Dolphin, D. *Bioorg. Med. Chem.* **1994**, *2*, 735−742.

DOI: 10.1021/jacs.6b04144
J. Am. Chem. Soc. 2016, 138, 8900−8911

(g) Kuroda, K.; Nakagawa-izumi, A. *Org. Geochem.* **2006**, *37*, 665−673. (h) Kuroda, K.; Nakagawa-izumi, A.; Dimmel, D. R. *J. Agric. Food Chem.* **2002**, *50*, 3396−3400.
(11) Isolation of *β*-5 compounds from lignin: (a) Lundquist, K.; Ericsson, L.; Karlsson, S.; Solymosy, F.; Shimizu, A. *Acta Chem. Scand.* **1970**, *24*, 3681−3686. Isolation of *β*-*β* derived compounds from lignin: (b) Lundquist, K.; Sydberger, T.; Bjerrum, J.; Nielsen, P. H.; Rasmussen, S. E.; Sunde, E.; Sørensen, N. A. *Acta Chem. Scand.* **1970**, *24*, 889−907. (c) Freudenberg, K.; Chen, C. L.; Harkin, J. M.; Nimz, H.; Renner, H. *Chem. Commun.* **1965**, *11*, 224−225.
(12) (a) Forsythe, W. G.; Garrett, M. D.; Hardacre, C.; Nieuwenhuyzen, M.; Sheldrake, G. N. *Green Chem.* **2013**, *15*, 3031−3038. (b) Lancefield, C. S.; Westwood, N. J. *Green Chem.* **2015**, *17*, 4980−4990. (c) Kishimoto, T.; Uraki, Y.; Ubukata, M. *Org. Biomol. Chem.* **2005**, *3*, 1067−1073.
(13) (a) Yue, F.; Lu, F.; Sun, R.; Ralph, J. *Chem. - Eur. J.* **2012**, *18*, 16402−16410. (b) Reale, S.; Attanasio, F.; Spreti, N.; De Angelis, F. *Chem. - Eur. J.* **2010**, *16*, 6077−6087. (c) Landucci, L. L.; Ralph, S. A. *J. Wood Chem. Technol.* **2001**, *21*, 31−52.
(14) (a) Deuss, P. J.; Scott, M.; Tran, F.; Westwood, N. J.; de Vries, J. G.; Barta, K. *J. Am. Chem. Soc.* **2015**, *137*, 7456−7467. (b) Scott, M.; Deuss, P. J.; de Vries, J. G.; Prechtl, M. H. G.; Barta, K. *Catal. Sci. Technol.* **2016**, *6*, 1882−1891.
(15) Buendia, J.; Mottweiler, J.; Bolm, C. *Chem. - Eur. J.* **2011**, *17*, 13877−13882.
(16) Pieters, L.; Van Dyck, S.; Gao, M.; Bai, R.; Hamel, E.; Vlietinck, A.; Lemière, G. *J. Med. Chem.* **1999**, *42*, 5475−5481.
(17) Lemiere, G.; Gao, M.; De Groot, A.; Dommisse, R.; Lepoivre, J.; Pieters, L.; Buss, V. *J. Chem. Soc., Perkin Trans. 1* **1995**, *13*, 1775−1779.
(18) (a) Cotelle, P.; Vezin, H. *Tetrahedron Lett.* **2003**, *44*, 3289−3292. (b) Orlandi, M.; Rindone, B.; Molteni, G.; Rummakko, P.; Brunow, G. *Tetrahedron* **2001**, *57*, 371−378. (c) Bolzacchini, E.; Brunow, G.; Meinardi, S.; Orlandi, M.; Rindone, B.; Rummakko, P.; Setala, H. *Tetrahedron Lett.* **1998**, *39*, 3291−3294.
(19) Lundquist, K.; Langer, V.; Li, S.; Stomberg, R. *Int. Symp. Wood Pulping Chem., 12th* **2003**, *1*, 239−244.
(20) A modification of the methodology of Lemiere et al.[17] allowed significantly less methyl iodide to be used whilst maintaining K_2CO_3 as base with only a slight decrease in yield (Table S1). An unexpected but interesting outcome was that by just changing the base to Cs_2CO_3 the ring-opened product **S1** was produced in 98% yield (Supporting Information section 4.0).
(21) Ireland, R. E.; Wipf, P.; Armstrong, J. D. *J. Org. Chem.* **1991**, *56*, 650−657.
(22) Patra, A.; Batra, S.; Bhaduri, A. P. *Synlett* **2003**, *11*, 1611−1614.
(23) (a) Lundquist, K.; Malmsten, L.-A.; Seip, H. M.; Pajunen, P.; Koskikallio, J.; Swahn, C.-G. *Acta Chem. Scand.* **1973**, *27*, 2597−2606. (b) Hibbert, H. *Annu. Rev. Biochem.* **1942**, *11*, 183−202. (c) Hibbert, H. *J. Am. Chem. Soc.* **1939**, *61*, 725−731. (d) Cramer, A. B.; Hunter, M. J.; Hibbert, H. *J. Am. Chem. Soc.* **1938**, *60*, 2813−2813. (e) Lundquist, K.; Hedlund, K.; Rasmussen, S. E.; Svensson, S.; Koskikallio, J.; Kachi, S. *Acta Chem. Scand.* **1971**, *25*, 2199−2210. (f) Lundquist, K.; Kirk, T. K.; Fredlund, F.; Beronius, P.; Engebretsen, J. E.; Ehrenberg, L. *Acta Chem. Scand.* **1971**, *25*, 889−894. (g) Lundquist, K.; Hedlund, K.; Svensson, S.; Norin, T.; Eriksson, G.; Blinc, R.; Paušak, S.; Ehrenberg, L.; Dumanović, J. *Acta Chem. Scand.* **1967**, *21*, 1750−1754. (h) Lundquist, K.; Ericsson, L.; Schroll, G.; Lindberg, A. A.; Lagerlund, I.; Ehrenberg, L. *Acta Chem. Scand.* **1971**, *25*, 756−758.
(24) (a) Sturgeon, M. R.; Kim, S.; Lawrence, K.; Paton, R. S.; Chmely, S. C.; Nimlos, M.; Foust, T. D.; Beckham, G. T. *ACS Sustainable Chem. Eng.* **2014**, *2*, 472−485. (b) Yokoyama, T. *J. Wood Chem. Technol.* **2014**, *35*, 27−42. (c) Harms, R. G.; Markovits, I. I. E.; Drees, M.; Herrmann, W. A.; Cokoja, M.; Kühn, F. E. *ChemSusChem* **2014**, *7*, 429−434. (d) Kaiho, A.; Kogo, M.; Sakai, R.; Saito, K.; Watanabe, T. *Green Chem.* **2015**, *17*, 2780−2783. (e) Jia, S.; Cox, B. J.; Guo, X.; Zhang, Z. C.; Ekerdt, J. G. *ChemSusChem* **2010**, *3*, 1078−1084.
(25) (a) West, E.; MacInnes, A. S.; Hibbert, H. *J. Am. Chem. Soc.* **1943**, *65*, 1187−1192. (b) Karlsson, O.; Lundquist, K.; Meuller, S.; Westlid, K.; Lönnberg, H.; Berg, J.-E.; Bartók, M.; Pelczer, I.; Dombi, G. *Acta Chem. Scand.* **1988**, *42b*, 48−51.
(26) (a) Lundquist, K. *Appl. Polym. Symp.* **1976**, *28*, 1393−1407. (b) Ito, H.; Imai, T.; Lundquist, K.; Yokoyama, T.; Matsumoto, Y. *J. Wood Chem. Technol.* **2011**, *31*, 172−182.
(27) Cox, B. J.; Jia, S.; Zhang, Z. C.; Ekerdt, J. G. *Polym. Degrad. Stab.* **2011**, *96*, 426−431.
(28) Li, S.; Lundquist, K. *Holzforschung* **1999**, *53*, 39−42.
(29) Jo, G.; Hyun, J.; Hwang, D.; Lee, Y. H.; Koh, D.; Lim, Y. *Magn. Reson. Chem.* **2011**, *49*, 374−377.
(30) Gardner, J. A. F. *Can. J. Chem.* **1954**, *32*, 532−537.
(31) (a) Huang, X.; Atay, C.; Korányi, T. I.; Boot, M. D.; Hensen, E. J. M. *ACS Catal.* **2015**, *5*, 7359−7370. (b) Saisu, M.; Sato, T.; Watanabe, M.; Adschiri, T.; Arai, K. *Energy Fuels* **2003**, *17*, 922−928.
(32) Anfimov, A. N.; Erdyakov, S. Y.; Gurskii, M. E.; Bubnov, Y. N. *Russ. Chem. Bull.* **2011**, *60*, 2336−2342.
(33) Bauer, S.; Sorek, H.; Mitchell, V. D.; Ibáñez, A. B.; Wemmer, D. E. *J. Agric. Food Chem.* **2012**, *60*, 8203−8212.
(34) Tanahashi, M.; Takeachi, H.; Higuchi, T. *Wood Res.* **1976**, *61*, 44−53.
(35) Schutyser, W.; Van den Bosch, S.; Renders, T.; De Boe, T.; Koelewijn, S.-F.; Dewaele, A.; Ennaert, T.; Verkinderen, O.; Goderis, B.; Courtin, C. M.; Sels, B. F. *Green Chem.* **2015**, *17*, 5035−5045.

DOI: 10.1021/jacs.6b04144
J. Am. Chem. Soc. 2016, 138, 8900−8911